Physica A 589 (2022) 126520

Contents lists available at ScienceDirect

Physica A

journal homepage: www.elsevier.com/locate/physa

Dynamics of node influence in network growth models ☆

Shravika Mittal [a,*], Tanmoy Chakraborty [a], Siddharth Pal [b]

[a] Department of CSE, IIIT-Delhi, India
[b] Raytheon BBN Technologies, USA

ARTICLE INFO

Article history:
Received 21 March 2021
Received in revised form 24 September 2021
Available online 19 October 2021

Keywords:
Network growth models
Node dynamics
Barabasi–Albert graphs
Fitness based models
Spatial models

ABSTRACT

Many classes of network growth models have been proposed in the literature for capturing real-world complex networks. Existing research primarily focuses on global characteristics of these models, e.g., degree distribution. We aim to shift the focus towards studying the network growth dynamics from the perspective of individual nodes. In this paper, we study how a metric for node influence in network growth models behaves over time as the network evolves. This metric, which we call node visibility, captures the probability of the node to form new connections. First, we conduct an investigation on three popular network growth models — preferential attachment, additive, and multiplicative fitness models; and primarily look into the "influential nodes" or "leaders" to understand how their visibility evolves over time. Subsequently, we consider a generic fitness model and observe that the multiplicative model strikes a balance between allowing influential nodes to maintain their visibility, while at the same time making it possible for new nodes to gain visibility in the network. Finally, we observe that a spatial growth model with multiplicative fitness can curtail the global reach of influential nodes, thereby allowing the emergence of a multiplicity of "local leaders" in the network.

1. Introduction

Over the past two decades, complex networks have been used to model real-world systems across different domains ranging from social, biological, information, and technological systems [1,2]. Investigating the behavior of influential entities or leaders in these real-world networks would help us understand how they are able to gather and maintain prominence over time. For instance, influential papers in citation networks continue to acquire new citations every year [3,4]. Likewise, celebrities in online social networks keep increasing their follower count over time. These influential entities act as potential spreaders of information in networks. Therefore, keeping a track of their characteristics in an evolving network could have significance in applications ranging from viral marketing and target advertisement to rumor and epidemic control, and protection from spam attacks [5–7]. To understand and model the dynamics of how a leader node maintains its influence over time, one needs to study the temporal behavior of nodes in a network.

In this paper, we introduce a notion, called *visibility of a node* which is defined as the *probability of the node to form new connections in a growing network*. For instance, in a preferential attachment model [8,9], the visibility of a node is proportional to its degree, and inversely proportional to the number of edges in the network. An essential aspect

☆ This document does not contain technology or technical data controlled under either the U.S. International Traffic in Arms Regulations or the U.S. Export Administration Regulations.

* Corresponding author.
E-mail addresses: shravika16093@iiitd.ac.in (S. Mittal), tanmoy@iiitd.ac.in (T. Chakraborty), siddharth.pal@raytheon.com (S. Pal).

https://doi.org/10.1016/j.physa.2021.126520
0378-4371/

of the study is to investigate the *visibility profile* of a node which characterizes the temporal evolution of the node's influence as the network grows. We argue that studying the visibility profile of nodes leads to a better understanding of network evolution due to attachment dynamics, which might not be possible to obtain by simply analyzing global network properties such as degree distribution or local node-centric properties such as degree, clustering coefficient, etc. Similar to node persistence over time studied in [10], our approach allows to make headway into this understanding by characterizing the *visibility behavior of leaders* in the network. While the framework is applicable to arbitrary nodes as well, it is more interesting to first understand the leaders' behavior. Chakraborty et al. [4] argued that the growth of the degree of a node (its visibility) in a citation network follows one of the five patterns — early rise, late rise, frequent rise, steady rise and steady drop. In a subsequent study [11], they also concluded that highly-cited papers and authors (leaders) follow steady rising pattern. However, it was not clear whether existing network growth models are able to describe such patterns particularly for leader nodes [12]. This motivates us to study the temporal evolution of the visibility of nodes, in particular leaders in networks generated by different network growth models.

We study the visibility of influential nodes[1] in the graphs simulated by the following network growth models. Barabási–Albert (BA) model [9], also known as the preferential attachment model, was able to explain power law behavior in real-world networks using the idea of network growth and the "rich-get-richer" phenomenon. However, the BA model could only capture the "old-get-rich" phenomenon or the "first-mover-advantage" whereby older nodes increase their connectivity and become dominant at the expense of younger nodes in the network. It does not take into account the competitive characteristics of a node that help them flourish in a very short period of time [13,14]; for instance, in citation networks a few research papers are able to gain lot of citations within a short span of time [15]. Using this as a motivation, Bianconi and Barabási [16,17] introduced a new class of network growth models in which the incoming nodes form connections based on inherent characteristics of nodes such as novelty, usefulness, etc., captured through a fitness value [18–23]. This was inspired by the "fit-get-richer" phenomenon observed in real-world networks [16]. Following this, Ergun and Rodgers [24] analyzed the degree distribution of network growth models with an attachment mechanism combining the degree and fitness information of nodes in an additive and multiplicative manner. While the additive model was found to exhibit a power law behavior similar to the BA model, the multiplicative model exhibited multiscaling, i.e., the power law behavior with parameter dependent on the fitness at a particular site.

There are several real-world networks in which the aspect of *space* plays an important role to understand dynamics of network evolution. For instance, in the biological domain the regions in brain that are spatially closer have a higher probability of being connected as compared to the far-off regions [25]. Similar significance of space can also be observed in online social networks capturing spatial features [26,27], transportation networks [28], and communication networks. To model networks incorporating spatial features, the class of spatial network models has been proposed. A basic spatial model incorporating notions of preferential and spatial attachment was proposed by Yook et al. [29] to capture underlying mechanisms driving the evolution of the Internet topology. Subsequently, Kaiser et al. [30] analyzed a spatial growth model where the edge connection probability decreases with node distance either in an exponential or a power-law manner to explain multiple, interconnected clusters that emerge in real-world networks. Barthélemy [31] noted that the spatial growth model with exponential decay with distance exhibited power law behavior with cutoff at high degree values. This was argued to have been observed due to distance effects limiting the choice of available connections. Furthermore, clustering, a phenomenon that does not occur in the BA or the fitness models, was observed in spatial models due to the fact that nodes that are closer in space, are more likely to be connected among themselves. See Barthélemy [32] for a comprehensive study on spatial networks. Recently, we proposed a new spatial growth model [12] that was better able to capture the five growth patterns presented in [4], compared to the preferential attachment model and its variants (i.e., additive and multiplicative fitness models [19,33]).

Defining the notion of visibility as a node metric in the context of network growth models is a key contribution of the present work. While the metric had been defined for the BA and the fitness models in our previous works [12,34], we extend the definition to spatial models as well. Defining a local metric that captures the visibility of a node gives us the tools and vocabulary to study their temporal behavior and how their level of influence might change over time. In contrast to existing literature that has mostly focused on global network-wide behavior in the large graph limit, our primary interest has been the local behavior of influential nodes over time. In the context of specific network models, we also describe conditions under which influential nodes might increase or decrease their visibility. Comparing and contrasting different network models and studying how influential nodes behave in each is a novel aspect of our work.

We extend our previous studies [12,34] and address the following problem statement: *Given an influential node with high visibility at a certain point in time, how would its visibility evolve over time*? This in itself is a novel and an interesting question in the context of network growth models. We investigate across three popular and diverse network growth models — Barabási–Albert (BA) model, (additive, multiplicative, and general) fitness based model and spatial models. One of the primary theoretical findings that we continue to build on from our previous work [34] is that leaders are able to gain more visibility in the multiplicative fitness model setting as compared to the BA and additive fitness models. Although, the "rich-get-richer" phenomenon [9] holds for both the BA and the AF models at the global scale in the large graph limit, "rich" or influential nodes at any given point in time are noted to lose global influence over time since the number

[1] We use "leaders" and "influential nodes" interchangeably to denote high-degree and/or high-fitness nodes that can keep attracting new edges over long periods of time.

of connections they attract cannot keep pace with the network growth. On the other hand, in the multiplicative fitness model, the influential nodes are able to increase their visibility over time, given that their fitness value remains high in comparison to the rest of the network; while, the visibility values always decrease over time for the BA and additive fitness models (see Section 3 for details). In Section 3.1, we study a general framework of fitness models and observe that a superlinear attachment rule based on degree and fitness would lead to highly dominant nodes and make it exceedingly difficult for new nodes to gain influence in the network. While this observation has relationship to the "winner-takes-all" [17,35] behavior reported in the context of multiplicative and superlinear models in the large graph limit, it must be noted that in the multiplicative model, a "winner" could be overtaken by a new node, which gets exceedingly difficult for the superlinear model. Experimental analysis provided in Section 4 supports our theoretical analysis that suggest multiplicative fitness models best explain the prolonged influence of leader nodes in certain real-world networks, while at the same time allowing new high fitness nodes to gain influence over time. However, we observe that multiplicative fitness models do not allow multiple influential nodes to exist at the same time. In Section 5, we investigate relationship between several concepts of visibility for spatial models, and give theoretical insights on how spatial growth models can allow a multiplicity of leaders to coexist while describing conditions under which local leaders could maintain or grow their influence; Section 6 provides experimental justifications for the same.

Reproducibility: To encourage reproducible research, the codes are publicly available at https://github.com/mittalshravika/Network-Growth-Models.

2. Network growth models

Following our previous work [34], here we set up the notations and problem definition. Consider the following sequence of graphs $\{\mathbb{G}_t,\ t = 0, 1, \ldots\}$, where $\mathbb{G}_t = (V_t, \mathbb{E}_t)$, with V_t and $\mathbb{E}_t$ being the set of nodes and edges in $\mathbb{G}_t$ respectively. In a network growth model, we have $V_t \subset V_{t+1}$ and $\mathbb{E}_t \subseteq \mathbb{E}_{t+1}$ for every $t = 0, 1, \ldots$. In other words, new nodes arrive at every time step t, and form connections with existing nodes, thus adding to the edge set of the previous graph $\mathbb{G}_{t-1}$. For purposes of simplicity, here we consider the basic model where a single node enters at any time step t, and forms a connection with one node in the existing graph $\mathbb{G}_{t-1}$. Therefore, we can label the incoming node by the time index of its entry to the network, which leads to $V_t = \{0, 1, \ldots, t\}$ for $t = 0, 1, \ldots$. Note that all our results can be easily extended to more general scenarios where multiple nodes can enter the network and incoming nodes can form multiple connections. At time t, let the degree of the node i in V_t be denoted by $D_t(i)$. Also, let the rv S_{t+1} denote the node with which an incoming node $t + 1$ connects.

Barabási–Albert (BA) model: In the preferential attachment mechanism [9], new nodes connect preferentially to existing nodes with higher degree. Let $\mathbf{p}^{BA}(t+1) = (p_i^{BA}(t+1),\ i \in V_t)$ be the pmf with which the new node indexed as $t + 1$ connects with the existing graph $\mathbb{G}_t$, i.e., $p_i^{BA}(t+1)$ is the probability with which node $t + 1$ connects with an existing node i. This is given by:

$$p_i^{BA}(t+1) = \mathbf{P}\left[S_{t+1} = i \mid \mathbb{G}_t\right] = \frac{D_t(i)}{\sum_{j\in V_t} D_t(j)},\ i \in V_t. \tag{1}$$

Note that we term node i's *visibility* in the graph $\mathbb{G}_t$ by $p_i^{BA}(t+1)$.

Fitness based attachment rules: In fitness based models [16,24,36], every node is assumed to have a fitness value independently drawn from a distribution, and new nodes connect preferentially on the basis of the fitness and degree values of the existing nodes. We describe multiple ways in which such an attachment could occur.

Assume a sequence of i.i.d. fitness rvs $(\xi, \xi_i,\ i = 0, 1, \ldots)$ with ξ_i denoting the fitness value of node i. A generic fitness model can be described by the following attachment rule

$$p_i^{GF}(t+1) = \frac{g(\xi_i, D_t(i))}{\sum_{j\in V_t} g(\xi_j, D_t(j))},\ i \in V_t, \tag{2}$$

for an attachment function $g : \mathbb{R} \times \mathbb{R} \to \mathbb{R}$ which determines the relative importance of the fitness and degree values. In the additive fitness model, new nodes connect preferentially to existing nodes having a higher sum of degree and fitness value. For $t = 0, 1, \ldots$, let the pmf delineating formation of new connections at time $t + 1$ be given by $\mathbf{p}^{AF}(t+1)$, where

$$p_i^{AF}(t+1) = \frac{\xi_i + D_t(i)}{\sum_{j\in V_t}(\xi_j + D_t(j))},\ i \in V_t. \tag{3}$$

Similarly, the attachment rule for multiplicative fitness (MF) model is given by

$$p_i^{MF}(t+1) = \frac{\xi_i \cdot D_t(i)}{\sum_{j\in V_t} \xi_j \cdot D_t(j)},\ i \in V_t. \tag{4}$$

Therefore, the *visibilities* of node i in graph $\mathbb{G}_t$ are given by $p_i^{AF}(t+1)$ and $p_i^{MF}(t+1)$ for the additive and multiplicative fitness models, respectively. Note that the influential nodes as described in Section 1 relate to nodes having high visibility as defined for the particular network growth model in question. On the other hand, "hubs" are referred to high degree nodes. Note that nodes could be influential or highly visible in the fitness models even before they become hubs. Likewise, hubs that were influential previously could be less visible at any point in time.

Spatial attachment rules: In spatial models [29,30,37], every node is assumed to have a location vector drawn from a distribution over a location space A. Assume a sequence of i.i.d. location rvs $(\chi,\ \chi_i,\ i = 0, 1, \ldots)$ and i.i.d. fitness rvs $(\xi, \xi_i,\ i = 0, 1, \ldots)$ with χ_i and ξ_i denoting the location and fitness values of node i respectively. A generic spatial attachment model can be given by the following attachment rule

$$p_i^{AT}(t+1) = \frac{h(\chi_i, \chi_{t+1}; \xi_i, D_i(t))}{\sum_{j\in V_t} h(\chi_j, \chi_{t+1}; \xi_j, D_j(t))}. \tag{5}$$

The attachment probability now depends on the location vector of the new node χ_{t+1}. This is different from the models described previously. Therefore, we could have multiple definitions of visibility. A global variant of visibility is given below

$$p_i^{\text{global}}(t+1) = \mathbb{E}_\chi\left[\frac{h(\chi_i, \chi; \xi_i, D_i(t))}{\sum_{j\in V_t} h(\chi_j, \chi; \xi_j, D_j(t))}\right], \tag{6}$$

while a local version is given as

$$p_i^{\text{local}}(t+1) = \frac{h(\chi_i, \chi_i; \xi_i, D_i(t))}{\sum_{j\in V_t} h(\chi_j, \chi_i; \xi_j, D_j(t))}, \tag{7}$$

where $h : A \times A \times \mathbb{R} \times \mathbb{N} \to \mathbb{R}$. We find it useful to consider the following separable form of attachment function

$$h(\chi_1, \chi_2; \xi_1, D_1) = \alpha(\chi_1, \chi_2)\beta(\xi_1, D_1),\ \ \chi_1, \chi_2 \in A, \tag{8}$$

where $\alpha : A \times A \to \mathbb{R}$ and $\beta : \mathbb{R} \times \mathbb{N} \to \mathbb{R}$. While the notion of global visibility models the overall attractivity of a node in the entire attribute space, the local visibility considers only its attractivity from the local neighborhood in the attribute space of a node. This model allows for nodes whose global attractivity is low, with their local attractivity being high.

3. Analytical results on node visibility – BA and fitness models

In this section, we study and compare the evolution of visibility of a node over time for the BA model and two fitness models, namely the additive and multiplicative fitness models. Results stated in Theorem 3.1 have appeared in our previous work (Lemma 2, [34]). The following theorem describes the change in visibility with time for the three growth models.

First, we introduce some notation: Define $\Xi_t = \sum_{i\in V_t} \xi_i$ and $\psi_t = \sum_{i\in V_t} \xi_i D_t(i)$, for $t = 0, 1, \ldots$. For any event $\mathcal{E}$, the indicator function $\mathbf{1}[\mathcal{E}] = 1$, when the event is true, and $\mathbf{1}[\mathcal{E}] = 0$ when the event does not hold.

Theorem 3.1. *For every $t = 0, 1, \ldots$, and i in V_{t-1}: Let $\mathbb{G}_{t-1}$ be the graph at time $t-1$, we have*

(i)

$$\mathbb{E}\left[p_i^{BA}(t+1) - p_i^{BA}(t) \mid \mathbb{G}_{t-1}\right] = -\frac{D_{t-1}(i)}{4t(t-1)}, \tag{9}$$

(ii)

$$\mathbb{E}\left[p_i^{AF}(t+1) - p_i^{AF}(t) \mid \mathbb{G}_{t-1}, \xi_t\right] = -\frac{(\xi_i + D_{t-1}(i))\,(\xi_t + 1)}{(\Xi_{t-1} + 2(t-1))\,(\Xi_t + 2t)}, \tag{10}$$

(iii)

$$\mathbb{E}\left[p_i^{MF}(t+1) - p_i^{MF}(t) \mid \mathbb{G}_{t-1}, \xi_t\right] \gtrsim \xi_i D_{t-1}(i)\frac{\sum_{j\neq i} \xi_j D_t(j)\left[\xi_i - \xi_t - \xi_j\right]}{\psi_{t-1}^2(\psi_{t-1} + \xi_i + \xi_t)}. \tag{11}$$

Proof. Fix $t = 0, 1, \ldots$, and i in V_t.

Preferential Attachment model: The difference in the visibility of node i in the BA model between time $t+1$ and t is given as

$$p_i^{BA}(t+1) - p_i^{BA}(t) = \frac{D_t(i)}{2t} - \frac{D_{t-1}(i)}{2(t-1)} = \frac{D_{t-1}(i) + \mathbf{1}[S_t = i]}{2t} - \frac{D_{t-1}(i)}{2(t-1)}. \tag{12}$$

The above follows by noting that the sum of degree rvs $D_t(i)$ for all the nodes in the vertex set V_t equals $2t$. Furthermore, by noting that when looking at the expected difference in visibility conditioned on the graph at time $t-1$, S_t is the only random variable in (12), we obtain

$$\mathbb{E}\left[p_i^{BA}(t+1) - p_i^{BA}(t) \mid \mathbb{G}_{t-1}\right] = \frac{D_{t-1}(i) + \mathbf{P}[S_t = i \mid \mathbb{G}_{t-1}]}{2t} - \frac{D_{t-1}(i)}{2(t-1)} \tag{13}$$

and (9) follows.

Additive Fitness model: Similarly in the additive fitness model, the difference in the visibility of node i can be written as

$$p_i^{AF}(t+1) - p_i^{AF}(t) = \frac{\xi_i + D_t(i)}{\sum_{j\in V_t}(\xi_j + D_t(j))} - \frac{\xi_i + D_{t-1}(i)}{\sum_{j\in V_{t-1}}(\xi_j + D_{t-1}(j))}$$
$$= \frac{\xi_i + D_{t-1}(i) + \mathbf{1}[S_t = i]}{\Xi_{t-1} + \xi_t + 2t} - \frac{\xi_i + D_{t-1}(i)}{\Xi_{t-1} + 2(t-1)}. \tag{14}$$

Taking expectation on both sides conditioned on $\mathbb{G}_{t-1}$ and ξ_t leads to the result

$$\mathbb{E}\left[p_i^{AF}(t+1) - p_i^{AF}(t) \mid \mathbb{G}_{t-1}, \xi_t\right] = -\frac{(\xi_i + D_{t-1}(i))\,(\xi_t + 1)}{(\Xi_{t-1} + 2(t-1))\,(\Xi_t + 2t)}. \tag{15}$$

Observe that for large t, by Strong Law of Large Numbers, Ξ_t can be approximated as $t\mathbb{E}[\xi]$. Using this, we obtain for large t,

$$\mathbb{E}\left[p_i^{AF}(t+1) - p_i^{AF}(t) \mid \mathbb{G}_{t-1}, \xi_t\right] \sim -\frac{(\xi_i + D_{t-1}(i))\,(\xi_t + 1)}{t(t-1)\,(2 + \mathbb{E}[\xi])^2}. \tag{16}$$

Multiplicative Fitness model: The difference in the visibility of node i can be written for the multiplicative model as follows

$$p_i^{MF}(t+1) - p_i^{MF}(t) = \frac{\xi_i D_t(i)}{\sum_{j\in V_t}\xi_j D_t(j)} - \frac{\xi_i D_{t-1}(i)}{\sum_{j\in V_{t-1}}\xi_j D_{t-1}(j)}$$
$$= \frac{\xi_i\,[D_{t-1}(i) + \mathbf{1}[S_t = i]]}{\psi_{t-1} + \xi_{S_t} + \xi_t} - \frac{\xi_i D_{t-1}(i)}{\psi_{t-1}}. \tag{17}$$

Furthermore, we lower bound the expected change in visibility as follows

$$\mathbb{E}\left[p_i^{MF}(t+1) - p_i^{MF}(t) \mid \mathbb{G}_{t-1}, \xi_t\right] \tag{18}$$
$$= \xi_i\left[\frac{D_{t-1}(i)+1}{\psi_{t-1} + \xi_i + \xi_t} - \frac{D_{t-1}(i)}{\psi_{t-1}}\right]\mathbf{P}[S_t = i \mid \mathbb{G}_{t-1}, \xi_t] + \xi_i \sum_{\ell\neq i}\left[\frac{D_{t-1}(i)}{\psi_{t-1} + \xi_\ell + \xi_t} - \frac{D_{t-1}(i)}{\psi_{t-1}}\right]\mathbf{P}[S_t = \ell \mid \mathbb{G}_{t-1}, \xi_t] \tag{19}$$
$$\approx \xi_i\left[\frac{\psi_{t-1}\mathbf{P}[S_t = i \mid \mathbb{G}_{t-1}, \xi_t]}{\psi_{t-1}\,(\psi_{t-1} + \xi_i + \xi_t)} - \frac{D_{t-1}(i)}{\psi_{t-1}} \times \left[\sum_{\ell\neq i}\mathbf{P}[S_t = \ell \mid \mathbb{G}_{t-1}, \xi_t] \cdot \frac{\xi_\ell + \xi_t}{\psi_{t-1} + \xi_\ell + \xi_t}\right]\right] \tag{20}$$
$$\geq \xi_i\left[\frac{\xi_i D_{t-1}(i)}{\psi_{t-1}\,(\psi_{t-1} + \xi_i + \xi_t)} - \frac{D_{t-1}(i)}{\psi_{t-1}} \cdot \frac{\sum_{\ell\neq i}\xi_\ell D_{t-1}(\ell)(\xi_\ell + \xi_t)}{\psi_{t-1}^2}\right]$$
$$\simeq \xi_i D_{t-1}(i)\left[\frac{\xi_i\psi_{t-1} - \sum_{\ell\neq i}\xi_\ell D_{t-1}(\ell)(\xi_\ell + \xi_t)}{\psi_{t-1}^2(\psi_{t-1} + \xi_i + \xi_t)}\right], \tag{21}$$

and the result follows. ■

The approximation in Eq. (21) holds when $\psi_{t-1} \gg (\xi_i + \xi_t)$, which is expected to be true for sufficiently large values of t.

We observe from (12) that a node's visibility increases if it forms a new edge connection in the BA model. However, it is also evident from Theorem 3.1 that the visibility of the node decreases in expectation, in a manner that is directly proportional to its degree $D_{t-1}(i)$. This can be understood from the fact that higher degree nodes in the network have higher visibility values as a result of which, their decrease in visibility would be more as compared to nodes that have lower visibility values. This also concurs with previous results on the growth of node degrees in BA models. Barabási and Albert [9] noted that the degree of node k at time t behaves as $D_t(k) \sim \left(\frac{t}{k}\right)^{\frac{1}{2}}$. This implies that the visibility of node k at time t, $\frac{D_t(k)}{2t} \sim \frac{1}{2\sqrt{k}}\frac{1}{\sqrt{t}}$. Note that, one can also derive the expected reduction in node visibility from this result as stated in (9) of Theorem 3.1. Furthermore, we have $\frac{dD_t(k)}{dt} \sim \frac{D_t(k)}{2t}$, which explains the "rich-get-richer" phenomenon where higher degree nodes get connections at a larger rate compared to other nodes. Nevertheless, even for high degree nodes, the rate of degree increase does reduce over time. While older nodes do achieve high degree over time, our results indicate that it becomes progressively more difficult to add new connections that keeps pace with the growth of the network.

In the additive fitness model, we can infer from (14) that a node's visibility increases when it forms a new edge, provided $\Xi_{t-1} + 2(t-1) > (\xi_t + 2)[\xi_i + D_{t-1}(i)]$. This condition is expected to hold for large values of t, unless the fitness value ξ_t, or ξ_i, or both, are very large. Similar to the BA model, node visibility decreases in expectation, with the magnitude of decrease being directly proportional to the sum of degree and fitness values, and the fitness value of the new incoming node ξ_t. For large t, (16) shows that the additive fitness model behaves very similar to the BA model. This is supported by the result from Ergun and Rodgers [24] that the degree distribution of the AF model is also power law with parameter $2 + \mathbb{E}[\xi]$.

In contrast with the above, we can see from (11) that in expectation, for the MF model, the nodes are able to increase their visibility over time, given that their fitness value remains large with respect to the network. In addition to this, the expected change in visibility directly depends on the product of fitness and the present degree of the node, boosting the visibility of a leader much more as compared to the BA and additive fitness models. This suggests that the MF model is fundamentally very different from the BA model, and even the AF model. The difference in degree distribution was noted in [24], where the authors observed that the MF model gives rise to a multiscaling behavior [24], i.e., the fraction of nodes with a certain degree is dependent on the degree and the fitness value. The result in [24] indicates that high fitness nodes show power law behavior with a lower exponent, i.e., heavier tail, compared to nodes with low fitness. While previous works have looked at the degree statistics at a network-wide scale in the large graph limit, we investigate the properties from the perspective of individual nodes.

Note that we derive results for change in visibility values over a single time step. The results can be easily generalized to any fixed number of time steps.

3.1. Node visibility over time — General fitness model

We study the change in node visibility over time for a general fitness model described in (2). For ease of notation, we define $\Gamma_t = \sum_{i\in V_t} g(\xi_i, D_t(i))$ and $\Delta^g_{t,i} = g(\xi_i, D_{t-1}(i)+1) - g(\xi_i, D_{t-1}(i))$ for i in V_t and $t = 1, 2, \ldots$.

Theorem 3.2. *For every $t = 0, 1, \ldots$, and i in V_{t-1}: Let $\mathbb{G}_{t-1}$ be the graph at time $t-1$, we have*

$$\begin{aligned}&\mathbb{E}\left[p_i^{GF}(t+1) - p_i^{GF}(t) \mid \mathbb{G}_{t-1}, \xi_t\right]\\ &\simeq \left(\frac{g(\xi_i, D_{t-1}(i))}{\Gamma_{t-1}^2}\right)\left[\frac{g(\xi_i, D_{t-1}(i))}{\Gamma_{t-1}}\cdot\left(\Delta^g_{t,i} - g(\xi_t, 1)\right) + \sum_{k\neq i}\left(\frac{g(\xi_k, D_{t-1}(k))}{\Gamma_{t-1}}\right)\left(\Delta^g_{t,i} - \Delta^g_{t,k} - g(\xi_t, 1)\right)\right].\end{aligned} \tag{22}$$

Proof. The difference in the visibility of node i can be written as follows

$$p_i^{GF}(t+1) - p_i^{GF}(t) = \mathbb{E}\left[\frac{g(\xi_i, D_{t-1}(i) + \mathbf{1}[S_t = i])}{\sum_{j\in V_t} g(\xi_j, D_{t-1}(j) + \mathbf{1}[S_t = j])} - \frac{g(\xi_i, D_{t-1}(i))}{\sum_{j\in V_{t-1}} g(\xi_j, D_{t-1}(j))}\right]. \tag{23}$$

We further introduce the following notation for k in V_t, $\Omega_{t,k} = \mathbf{1}[S_t = k]$.

$$\begin{aligned}&p_i^{GF}(t+1) - p_i^{GF}(t)\\ &= \Omega_{t,i}\left[\frac{g(\xi_i, D_{t-1}(i)+1)}{\Gamma_{t-1} + \Delta^g_{t,i} + g(\xi_t, 1)} - \frac{g(\xi_i, D_{t-1}(i))}{\Gamma_{t-1}}\right] + \sum_{k\neq i}\Omega_{t,k}\left[\frac{g(\xi_i, D_{t-1}(i))}{\Gamma_{t-1} + \Delta^g_{t,k} + g(\xi_t, 1)} - \frac{g(\xi_i, D_{t-1}(i))}{\Gamma_{t-1}}\right].\end{aligned}$$

Furthermore, we introduce the following shorthand, $\hat{g}_{t,i} = g(\xi_i, D_{t-1}(i))$ and continue from above.

$$\begin{aligned}&p_i^{GF}(t+1) - p_i^{GF}(t)\\ &= \Omega_{t,i}\left[\frac{\sum_{\substack{j\neq i\\ j\in V_{t-1}}}\hat{g}_{t,j}\Delta^g_{t,i} - g(\xi_t, 1)\hat{g}_{t,i}}{\Gamma_{t-1}\left(\Gamma_{t-1} + \Delta^g_{t,i} + g(\xi_t, 1)\right)}\right] + \sum_{k\neq i}\Omega_{t,k}\left[\frac{-\hat{g}_{t,i}\Delta^g_{t,k} - g(\xi_t, 1)\hat{g}_{t,i}}{\Gamma_{t-1}\left(\Gamma_{t-1} + \Delta^g_{t,k} + g(\xi_t, 1)\right)}\right].\end{aligned} \tag{24}$$

Using expression (24), we approximate the expected change in visibility for sufficiently large values of t, as follows

$$\begin{aligned}&\mathbb{E}\left[p_i^{GF}(t+1) - p_i^{GF}(t) \mid \mathbb{G}_{t-1}, \xi_t\right]\\ &\simeq \mathbf{P}[S_t = i \mid \mathbb{G}_{t-1}, \xi_t]\left[\frac{\left(\sum_{\substack{j\neq i\\ j\in V_{t-1}}}\hat{g}_{t,j}\Delta^g_{t,i}\right) - g(\xi_t, 1)\hat{g}_{t,i}}{\Gamma_{t-1}^2}\right] - \sum_{k\neq i}\mathbf{P}[S_t = k \mid \mathbb{G}_{t-1}, \xi_t]\left[\frac{\hat{g}_{t,i}\Delta^g_{t,k}}{\Gamma_{t-1}^2} + \frac{g(\xi_t, 1)\hat{g}_{t,i}}{\Gamma_{t-1}^2}\right],\end{aligned} \tag{25}$$

and on substituting the expressions for $\{\mathbf{P}[S_t = \ell \mid \mathbb{G}_{t-1}, \xi_t],\ \ell \in V_{t-1}\}$, we obtain

$$\begin{aligned}&\simeq \frac{\hat{g}_{t,i}\Delta^g_{t,i}}{\Gamma_{t-1}^2} - \hat{g}_{t,i}\sum_{k\neq i}\frac{\hat{g}_{t,k}}{\Gamma_{t-1}}\frac{\Delta^g_{t,k}}{\Gamma_{t-1}^2} - \frac{g(\xi_t, 1)\hat{g}_{t,i}}{\Gamma_{t-1}^2}\\ &= \left(\frac{\hat{g}_{t,i}}{\Gamma_{t-1}^2}\right)\left[\Delta^g_{t,i} - \sum_{k\neq i}\frac{\hat{g}_{t,k}}{\Gamma_{t-1}}\Delta^g_{t,k} - g(\xi_t, 1)\right]\end{aligned}$$

$$= \left(\frac{\hat{g}_{t,i}}{\Gamma_{t-1}^2}\right)\left[\left(\frac{\hat{g}_{t,i}}{\Gamma_{t-1}}\right)\left(\Delta_{t,i}^g - g(\xi_t, 1)\right) + \sum_{k\neq i}\left(\frac{\hat{g}_{t,k}}{\Gamma_{t-1}}\right)\left(\Delta_{t,i}^g - \Delta_{t,k}^g - g(\xi_t, 1)\right)\right]. \quad \blacksquare$$

The approximations hold when

$$\Gamma_{t-1} \gg \Delta_{t,k}^g + g(\xi_t, 1),$$

and

$$\frac{\sum_{\substack{j\neq i \\ j\in V_{t-1}}} \hat{g}_{t,j}}{\Gamma_{t-1}} \approx 1.$$

The above conditions will hold for sufficiently large values of t. The expected change in visibility will be positive if

$$\Delta_{t,i}^g \geq \Delta_{t,k}^g, \ \ k \neq i, k \in V_{t-1},$$

and $\Delta_{t,i}^g \geq g(\xi_t, 1)$. While this is a sufficient condition, the expected change in visibility will be positive if node i has significantly large visibility in the network. Observe that for the BA and additive fitness models, $\Delta_{t,i}^g = 1$. While for the BA model, the approximation is too crude, we obtain a decrease in expected visibility for the additive model from (22). For the MF model,

$$\Delta_{t,i}^g = \xi_i(D_{t-1}(i) + 1) - \xi_i D_{t-1}(i) = \xi_i.$$

Therefore, $\Delta_{t,i}^g$ will be greater for nodes with higher fitness values. However, an incoming node with a high fitness value can lead to a decrease in the expected visibility of an influential node. This agrees with our findings in Theorem 3.1. For attachment functions which combine the fitness and degree information in a superlinear fashion, influential nodes can retain greater visibility for longer periods of time while being protected from decrease in visibility due to new nodes with high fitness values. For superlinear attachment rules, i.e., $g(\xi_i, D_t(i)) = (\xi_i D_t(i))^\alpha$, with $\alpha > 1$, we have

$$\begin{aligned}\Delta_{t,i}^g &= (\xi_i(D_{t-1}(i) + 1))^\alpha - (\xi_i D_{t-1}(i))^\alpha \\ &= \xi_i^\alpha D_{t-1}(i)^\alpha \left(\left[1 + \frac{1}{D_{t-1}(i)}\right]^\alpha - 1\right) \\ &\approx \alpha \xi_i^\alpha D_{t-1}(i)^{\alpha-1}, \end{aligned} \tag{26}$$

where the approximation is achieved by Taylor series, which will be accurate for large values of $D_{t-1}(i)$.

Observe that $\Delta_{t,i}^g$ is now a function of both the fitness and degree values. In such superlinear attachment rules, new nodes with high fitness values cannot lead to a decrease in expected visibility for influential nodes because of their low initial degree. Also, nodes with low degree and high fitness values could experience a decrease in their visibility because only nodes with significantly large fitness and degree values can increase their visibility in an expected sense, which is not the case for the multiplicative model. This would lead to a great difficulty for new nodes with high fitness values to attain visibility in the network. Furthermore, it will become progressively more difficult for new nodes to become visible in the network. In the experimental section, we will consider the special case of the quadratic scaling ($\alpha = 2$). In this setting, we have $\Delta_{t,i}^g = \xi_i^2\,(2D_t(i) + 1)$, which is very close to the expression (26) with $\alpha = 2$.

Thus with superlinear attachment rule, we expect a "winner-takes-all" behavior where an influential node will keep getting most of the connections over time. This is in accordance with previous result [35] that observed this behavior in the large graph limit with superlinear scaling on the degree information alone. However, in the MF model, while the "winner-takes-all" and the "fit-get-rich" behaviors are also observed [16] in the large graph limit, it is noted that a "winner" at a given point in time will not hinder the visibility growth of a newly introduced node with high fitness, and therefore can be potentially overtaken in the future by that node. This is demonstrated further through simulations in Section 4.

4. Experimental results on node visibility — Fitness models

In order to illustrate Theorems 3.1 and 3.2 and depict the change in visibility of influential nodes, we carry out two sets of simulation experiments. We compare how the visibility of leaders or influential nodes change over time in the Barabasi–Albert (BA), additive fitness (AF), multiplicative fitness (MF) and general fitness (GF) models. Throughout, the fitness variable ξ is taken to be Pareto distributed with parameter α_p having the following probability distribution,

$$p(\xi) = \alpha_p/\xi^{\alpha_p+1}, \ \ \xi \geq 1. \tag{27}$$

While our theoretical analysis is not dependent on the choice of fitness distribution, for the purpose of experimental study we choose power-law distributed fitnesses, because power-law distribution appear in many contexts when individuals are ranked according to certain feature of interest [38]. Furthermore, Pareto distributed fitnesses allows for interesting experimental study, since the statistics of the fitness distribution can vary greatly depending on the parameter of the

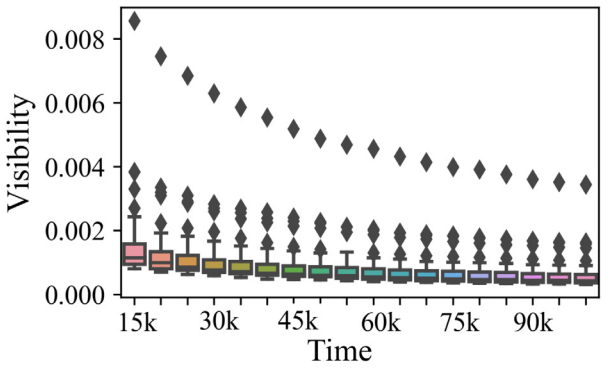

Fig. 1. Visibility of nodes (averaged over 50 independent runs) over time (after $T = 100000$ iterations) in the BA model. Observe that the visibility of influential nodes reduce with time as predicted by Theorem 3.1.

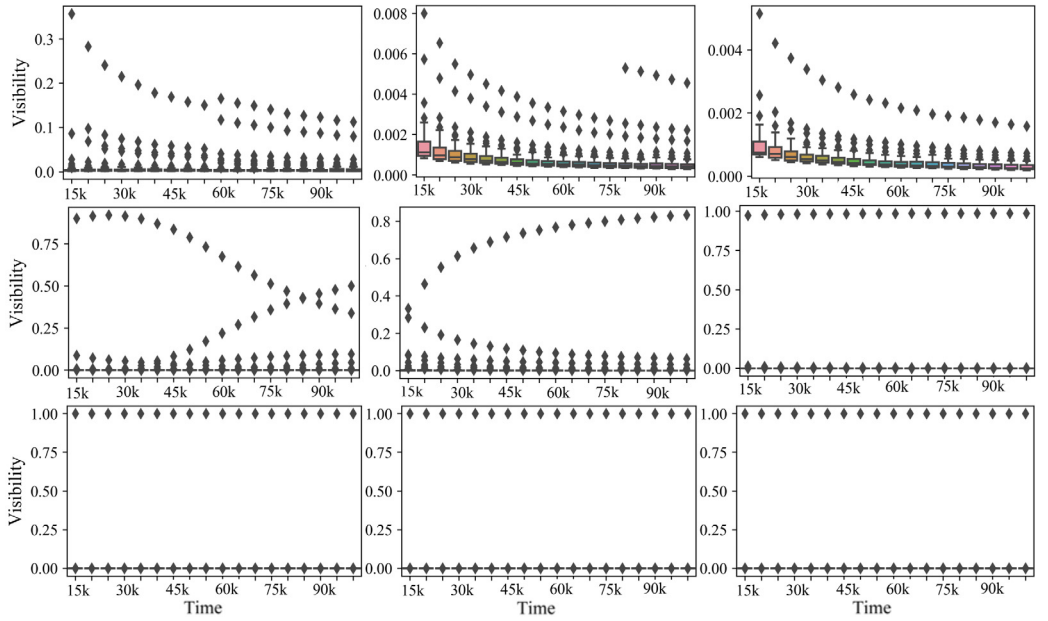

Fig. 2. Visibility of nodes (averaged over 50 independent runs) over time in three growth models. The columns represent different parameters of the Pareto distribution: $\alpha_p = 1, 2, 3$. Each row shows visibility results of the 50 most influential nodes after $T = 100000$ iterations for the three growth models — additive (AF), multiplicative (MF) and general fitness (GF) model. In the GF model, quadratic scaling is used, i.e., $\alpha = 2$; $g(\xi_i, D_t(i)) = (\xi_i D_t(i))^2$. Observe that the visibility of influential nodes reduce over time for the AF model. On the other hand, for the MF and GF models, the influential node maintains its visibility for extended periods of time. Note that later in time, a new node overtakes the highest visibility node in the multiplicative model, which does not occur in the GF model.

Pareto distribution. For $\alpha_p > 1$, the mean of the Pareto distribution is $\frac{\alpha_p}{\alpha_p - 1}$; while for $\alpha_p \leq 1$, the mean is infinite. For $\alpha_p > 2$, the variance is $\frac{\alpha_p}{(\alpha_p-1)^2(\alpha_p-2)}$; and for $\alpha_p \leq 2$, the variance is infinite. In other words, with $\alpha_p \leq 1$, the distribution is so heavy-tailed that both the mean and variance are infinite. With $\alpha_p = 2$, the distribution is less heavy-tailed, such that the mean is finite but the variance is still infinite. With $\alpha_p = 3$, the distribution has both a finite mean and variance. In our experimental analysis we show results for these three settings of α_p ($\alpha_p = 1, 2, 3$).

We use a quadratic attachment rule for general fitness model with $g(\xi_i, D_t(i)) = (\xi_i D_t(i))^2$.

For each given growth model and parameter value of the Pareto distribution, we generate a graph $\mathbb{G}^X_{T_0}$, where $X \in \{BA, AF, MF, GF\}$ and $T_0 = 10000$. We define $p_{(k)}(T_0; \mathbb{G}^X_t)$ to be the visibility of the node in graph $\mathbb{G}^X_t$ which had the k-highest visibility in graph $\mathbb{G}^X_{T_0}$. For each growth model, starting from $\mathbb{G}^X_{T_0}$, we generate R realizations $\mathbb{G}^{X,(1)}_T, \mathbb{G}^{X,(2)}_T, \ldots \mathbb{G}^{X,(R)}_T$ with $T = 100000$, which are mutually independent conditioned on $\mathbb{G}^X_{T_0}$. Since we are interested in the evolution of the visibility of influential nodes, for the purpose of this experiment we track the visibility of the top 50 nodes

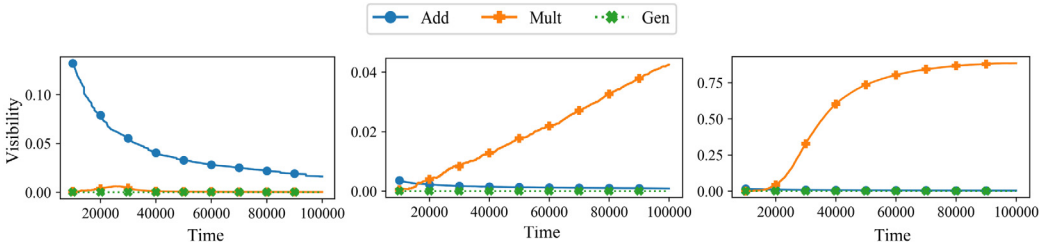

Fig. 3. Visibility of new node (averaged over 50 independent runs) added with a high fitness value over time in the three growth models – additive, multiplicative and general fitness model. This represents results for different parameters of the Pareto distribution: $\alpha_p = 1, 2, 3$. Observe that with for $\alpha_p = 2, 3$, the new node with high fitness value increases its visibility over time, which is not observed for the GF model.

starting from $t = 10000$ to $t = 100000$. However, conditioned on the graph at time T_0, the visibility values are random variables; therefore, we average the visibility values across all the realizations at any given time. We define $\bar{p}_{(k)}(T_0; t; X) = \frac{1}{R}\sum_{r=1}^{R} p_{(k)}(T_0; \mathbb{G}_t^{X,(r)})$ as the averaged visibility of the node at time t ($t > T_0$) which had the k-highest visibility at time T_0 for growth model X.

In other words, we track $p_{(k)}\left(T_0; \mathbb{G}_t^{X,(r)}\right)$ for $k = 1, 2, \ldots, 50$, $r = 1, 2, \ldots, R$, $t = 10000, 10001, \ldots, 100000$, and $X \in \{BA, AF, MF, GF\}$. For large enough independent runs R, we expect $\bar{p}_{(k)}(T_0; t; X)$ to be a reasonable approximation of $\mathbb{E}\left[p_{(k)}\left(T_0; \mathbb{G}_t^{X,(1)}\right) | \mathbb{G}_{T_0}^{X}\right]$, which is the expected value of visibility at time t for the node which had the k-highest visibility value at time T_0 conditioned on the graph at time T_0.

The box plots[2] in Figs. 1 and 2 show the change in visibility of top 50 nodes at $t = T_0 = 10000$ when the graph is allowed to grow for 90000 iterations until $t = 100000$. Visibility values averaged over $R = 50$ independent runs from $T_0 = 10000$ are shown. We observe from the two figures that the highest visibility nodes in the BA and AF slowly reduce in their visibility values over time as was predicted by Theorem 3.1. We can further characterize the decay in node visibility in these two model. Results from [9] show that $D_t(i) \sim \left(\frac{t}{i}\right)^{1/2}$, which leads to $p_i^{BA}(t) = \frac{D_t(i)}{2t} \sim \left(\frac{1}{2\sqrt{i}}\right) t^{-1/2}$. We also note from Theorem 3.1 that the change in visibility of node i between t+1 and t in the AF model can be rewritten as

$$\mathbb{E}\left[p_i^{AF}(t+1) - p_i^{AF}(t) \mid \mathbb{G}_{t-1}, \xi_t\right] = -\frac{p_i^{AF}(t)\,(\xi_t + 1)}{(\Xi_t + 2t)}. \tag{28}$$

Using Strong Law of Large Numbers we obtain the following approximation for large t

$$\mathbb{E}\left[p_i^{AF}(t+1) - p_i^{AF}(t) \mid \mathbb{G}_{t-1}, \xi_t\right] \sim -\frac{p_i^{AF}(t)\,(\xi_t + 1)}{t\,(2 + \mathbb{E}[\xi])}, \tag{29}$$

and upon applying expectation with respect to ξ_t, we obtain

$$\mathbb{E}\left[p_i^{AF}(t+1) - p_i^{AF}(t) \mid \mathbb{G}_{t-1}\right] \sim -\frac{p_i^{AF}(t)\,(\mathbb{E}[\xi] + 1)}{t\,(2 + \mathbb{E}[\xi])}. \tag{30}$$

The above implies that

$$\frac{dp_i^{AF}(t)}{p_i^{AF}(t)} \sim -\frac{(1 + \mathbb{E}[\xi])}{t\,(2 + \mathbb{E}[\xi])}dt$$

which in turn leads to the following approximation, $p_i^{AF}(t) \sim t^{-\frac{(1+\mathbb{E}[\xi])}{(2+\mathbb{E}[\xi])}}$. This implies that for the AF model the decay in visibility will be as $t^{-\theta}$, with $\frac{1}{2} < \theta < 1$. Observe that when $\mathbb{E}[\xi] = 0$, the visibility decays as $t^{-1/2}$ as would be expected in the BA model.

We also observe that many more nodes in BA and AF models have significantly higher visibility values compared to the average visibility value in their individual networks. However, for the multiplicative fitness model only 2 nodes exhibit high visibility values (for $\alpha_p = 1, 2$), with one node dominating the entire network at any point of time for most of the duration. In the MF model, for $\alpha_p = 1, 2$, we observe that a node with lower visibility replaces one with higher visibility between $t = T_0 = 10000$ and $t = 100000$, because the lower visibility node joined the network later but with

[2] The box plot graphically represents certain statistical properties of a dataset through their quartiles. Observe that boxes contain lines extending from itself (called whiskers), indicating variability outside the upper and lower quartiles. Outliers present in the data distribution are shown as individual data points (refer to points represented using diamonds in Figs. 1 and 2). The minimum and maximum values in the dataset (excluding outliers) corresponds to the lower and upper whiskers respectively. The first (Q_1) and the third (Q_3) quartiles are captured by the lower and upper end of the boxes, while the median is captured by a line within the box. In our plots, the lower whisker corresponds to the smallest data sample larger than $Q_1 - 1.5{*}$IQR and upper whisker corresponds to the largest data sample smaller than $Q_3 + 1.5{*}$IQR, where IQR represents Inter Quartile Range ($Q_3 - Q_1$). Data points lying beyond the lower and upper whiskers are considered as outliers.

a significantly higher fitness value. For $\alpha_p = 3$, we do not see this behavior because it is less likely that a node with a significantly high fitness value will enter the network. As a result, in contrast with BA and AF models, for the MF model we can see from (11) and Fig. 2 that in expectation, an influential node is able to increase its visibility over time, given that its fitness value remains large with respect to rest of the nodes in the network.

While we observe that in both the MF and GF models, nodes with high visibility are able to maintain their influence (or, visibility) over time, we next investigate how easy it is for new nodes with high fitness to gain influence over time. For this purpose, we conduct an experiment where we introduce a node at time $t = T_0 + 1 = 10001$, with fitness value $\xi_{T_0+1} = 2\max_{t\in V_{T_0}} \xi_t$, i.e., twice the fitness value of the maximum fitness value among all nodes until time T_0. For growth model $X \in \{AF, MF, GF\}$, we generate $R = 50$ realizations beyond time T_0 by setting the fitness value of node $T_0 + 1$ as mentioned above. We define $p_i\left(\mathbb{G}_t^X\right)$ to be the visibility of the node i in graph $\mathbb{G}_t^X$. We average the visibility values across R realizations, $\mathbb{G}_T^{X,(1)}, \mathbb{G}_T^{X,(2)}, \ldots, \mathbb{G}_T^{X,(R)}$, and compute the averaged visibility of node $T_0 + 1$ defined as $\bar{p}_{T_0+1}(t) = \frac{1}{R}\sum_{r=1}^{R}\left(\mathbb{G}_t^{X,(r)}\right)$, $t > T_0$. Subsequently, we track the visibility of this newly introduced node in the three fitness models and present the results in Fig. 3. We observe that in the AF and GF models, the visibility of the newly introduced node decreases with time. This concurs with Theorem 3.1 where we showed that the visibility of nodes in AF models decreases with time; and with Theorem 3.2 where we argue that in the general fitness model with a superlinear attachment rule, it becomes progressively difficult for new nodes to get visible in the network. For the MF model with $\alpha_p = 1$, we observe that $\bar{p}_{T_0+1}(t)$ increases slightly but decays beyond $t = 30000$. This is because nodes with even higher fitness values enter the network after node $T_0 + 1$. However, for $\alpha_p = 2, 3$ the visibility of node $T_0 + 1$ keeps increasing until $t = 100000$. Note that for $\alpha_p = 3$, node $T_0 + 1$ becomes dominant in the network very quickly because as the node increases its degree, the degree-fitness product becomes large compared to that of other nodes in the network because having a large fitness node is a rarer event for larger value of α_p.

From the experiments we reaffirm that multiplicative models allow high visibility nodes to maintain their influence in the network for a longer period of time, while at the same time allowing high fitness nodes that are introduced later in the network to become influential. However, we observe that only a few number of nodes can be influential in the network at any given moment of time. This leads us to consider spatial attachment rules in conjunction with the multiplicative model to enforce regions of influence for each individual node such that multiple influential nodes can coexist in a network at the same time.

5. Analytical results on node visibility — Spatial models

In the previous sections, we investigated the node visibility dynamics of the fitness models. A major takeaway was that multiplicative fitness models allow influential nodes to maintain their visibility while still permitting newly introduced nodes with high fitness to gain influence over time. However, a shortcoming of the MF model was that it could not support a multiplicity of influential nodes. We investigate whether a configuration of spatial models exists that retains the positive aspects of the MF model while addressing this shortcoming.

5.1. Preliminaries — results on various notions of visibility in spatial models

Having defined global (6) and local (7) visibilities for a node in Section 2, we find it helpful to define a notion of maximum visibility

$$p_i^{\max}(t+1) = \max_{\chi} \frac{h(\chi_i, \chi; \xi_i, D_i(t))}{\sum_{j\in V_t} h(\chi_j, \chi; \xi_j, D_j(t))}, \tag{31}$$

with $\chi_{t,i}^*$ being the location vector for which the maximum is attained. For rest of the analysis, we assume that the attachment function h is separable into a product form of $\alpha(\chi_1, \chi_2)\cdot\beta(\xi, D)$ as shown in (8). For analytical purposes, we set $\alpha(\chi_1, \chi_2) = e^{-\gamma d(\chi_1,\chi_2)}$, where $d : A \times A \to \mathbb{R}$ is a metric on the location space A.

Lemma 5.1. *For $\alpha(\chi_1, \chi_2) = e^{-\gamma d(\chi_1,\chi_2)}$ and every $t = 1, 2, \ldots$,*

$$\lim_{\gamma\to\infty} p_i^{local}(t+1) = 1 = \lim_{\gamma\to\infty} p_i^{max}(t+1) \tag{32}$$

and

$$\lim_{\gamma\to\infty} \chi_{t,i}^* = \chi_i. \tag{33}$$

In other words, for all $\delta > 0$ and for all $t = 1, 2, \ldots$, there exists $\gamma_{t,\delta}$ such that for all $\gamma \geq \gamma_{t,\delta}$

$$\left|p_i^{local}(t+1) - p_i^{max}(t+1)\right| < \delta$$

and

$$\left|\chi_i - \chi_{t,i}^*\right| < \delta.$$

Proof. For i in V_t and $t = 1, 2, 3, \ldots$

$$\begin{aligned} & p_i^{\text{local}}(t+1) \\ &= \frac{\beta(\xi_i, D_i(t))}{\beta(\xi_i, D_i(t)) + \sum_{j\neq i} e^{-\gamma d(\chi_i,\chi_j)}\beta(\xi_j, D_j(t))} \\ &\geq \frac{\beta(\xi_i, D_i(t))}{\beta(\xi_i, D_i(t)) + \left(t \max_{k\in V_t} \xi_k\right) \sum_{j\neq i} e^{-t^\epsilon d(\chi_i,\chi_j)}} \\ &\xrightarrow{\gamma = t^\epsilon \to \infty} 1 \end{aligned}$$

and we obtain first part of (32). Note that the scaling $\gamma = t^\epsilon$ implies that for larger graphs, a smaller γ would be necessary. Second part is obtained by noting that $p_i^{\max}(t+1) \geq p_i^{\text{local}}(t+1)$ for every node i and time t. Eq. (33) also follows similarly. ■

Lemma 5.1 suggests that $p_i^{\max}$ is a good approximation for p_i^{local} when γ is sufficiently large. Next, we derive relationships between the global and local notions of visibility.

Lemma 5.2. *For $\epsilon > 0$, we have*

$$\begin{aligned} & e^{-2\gamma\epsilon}\mathbf{P}\left[d(\chi, \chi_i) < \epsilon\right] p_i^{local}(t+1) \leq p_i^{global}(t+1) \\ & \leq p_i^{max}(t+1) \approx p_i^{local}(t+1). \end{aligned} \tag{34}$$

Proof. For convenience, we use the shorthand notation, $\beta_i(t) = \beta(\xi_i, D_i(t))$ for i in V_t and $t = 1, 2, \ldots$. The upper bound on $p_i^{\text{global}}(t+1)$ follows from the definition of $p_i^{\max}(t+1)$. To obtain the lower bound, for a fixed $\epsilon > 0$ we condition on the event $\mathbf{1}\left[d(\chi_i, \chi) < \epsilon\right]$

$$\begin{aligned} & p_i^{\text{global}}(t+1) \\ & \geq \mathbb{E}_\chi\left[\frac{h(\chi_i, \chi; \xi_i, D_i(t))}{\sum_{j\in V_t} h(\chi_j, \chi; \xi_j, D_j(t))}\mathbf{1}\left[d(\chi_i, \chi) < \epsilon\right]\right] \\ & \geq \mathbf{P}\left[d(\chi_i, \chi) < \epsilon\right] \cdot \min_{\chi: d(\chi,\chi_i)<\epsilon} \frac{h(\chi_i, \chi; \xi_i, D_i(t))}{\sum_{j\in V_t} h(\chi_j, \chi; \xi_j, D_j(t))} \\ & = \mathbf{P}\left[d(\chi_i, \chi) < \epsilon\right] \times \min_{\chi: d(\chi,\chi_i)<\epsilon} \frac{e^{-\gamma d(\chi,\chi_i)}\beta_i(t)}{e^{-\gamma d(\chi,\chi_i)}\beta_i(t) + \sum_{j\neq i} e^{-\gamma d(\chi,\chi_j)}\beta_j(t)} \\ & \geq \mathbf{P}\left[d(\chi_i, \chi) < \epsilon\right] \cdot \frac{e^{-2\gamma\epsilon}\beta_i(t)}{\beta_i(t) + \sum_{j\neq i} e^{-\gamma d(\chi_i,\chi_j)}\beta_j(t)} \\ & = e^{-2\gamma\epsilon}\mathbf{P}\left[d(\chi, \chi_i) < \epsilon\right] p_i^{\text{local}}(t+1), \end{aligned} \tag{35}$$

where the penultimate step follows from triangle inequality. ■

Lemma 5.2 gives a lower and upper bound for the global visibility in terms of the local visibility. As argued previously, since the model is more concerned with local attractivity of nodes, we will present analysis for p_i^{local}. Lemma 5.2 suggests that changes in the local visibility should also be aptly reflected in the global visibility.

5.2. Node visibility over time

For convenience, we define some shorthand notation: For i in V_t, $\beta_i(t) = \beta(\xi_i, D_i(t))$. For i, j in V_t, $\hat{h}_{t,i\to j} = h(\chi_i, \chi_j; \xi_i, D_{t-1}(i))$, $\hat{h}^+_{t,i\to j} = h(\chi_i, \chi_j; \xi_i, D_{t-1}(i)+1)$ represent the attachment function for node i at the location of node j, and $\Delta^h_{t,i\to j} = h(\chi_i, \chi_j; \xi_i, D_{t-1}(i)+1) - h(\chi_i, \chi_j; \xi_i, D_{t-1}(i))$. For k in V_t, $\Omega_{t,k} = \mathbf{1}\left[S_t = k\right]$ and $\Gamma_{t,k} = \sum_{i\in V_t} \hat{h}_{t,i\to k}$.

Theorem 5.3. *For every $t = 0, 1, \ldots$, and i in V_{t-1}: Let $\mathbb{G}_{t-1}$ be the graph at time $t-1$, we have*

$$\mathbb{E}\left[p_i^{local}(t+1) - p_i^{local}(t) \mid \mathbb{G}_{t-1}, \xi_t, \chi_t\right] \lesssim C_1 \sum_{k\in V_t} \beta_k(t-1) e^{-\gamma d(\chi_i,\chi_k)}\left\{\xi_i - e^{-\gamma d(\chi_i,\chi_k)}\xi_k - \xi_t\right\} \tag{36}$$

and

$$\mathbb{E}\left[p_i^{local}(t+1) - p_i^{local}(t) \mid \mathbb{G}_{t-1}, \xi_t, \chi_t\right] \gtrsim C_2 \sum_{k\in V_t} \beta_k(t-1) e^{-\gamma d(\chi_i,\chi_k)} \times \left\{\xi_i - e^{2\epsilon\gamma} e^{-\gamma d(\chi_i,\chi_k)}\xi_k - e^{3\epsilon\gamma}\xi_t\right\} \tag{37}$$

with

$$C_1 = \frac{1}{\left(\sum_{j\in V_t} h(\chi_j, \chi_i; \xi_j, D_{t-1}(j))^3\right)}\beta_i(t-1)$$

and

$$C_2 = \mathbf{P}\left[d(\chi_t, \chi) < \epsilon\right] e^{-\epsilon\gamma} \times \frac{1}{\left(\sum_{j\in V_t} h(\chi_j, \chi_i; \xi_j, D_{t-1}(j))^3\right)}\beta_i(t-1).$$

Proof. The difference in the local visibility of node i can be written as follows

$$\begin{aligned}
&p_i^{\text{local}}(t+1) - p_i^{\text{local}}(t)\\
&= \frac{h(\chi_i, \chi_i; \xi_i, D_{t-1}(i) + \mathbf{1}[S_t = i])}{\sum_{j\in V_t} h(\chi_j, \chi_i; \xi_j, D_{t-1}(j) + \mathbf{1}[S_t = j])} - \frac{h(\chi_i, \chi_i; \xi_i, D_{t-1}(i))}{\sum_{j\in V_{t-1}} h(\chi_j, \chi_i; \xi_j, D_{t-1}(j))}\\
&= \Omega_{t,i}\left[\frac{\hat{h}^+_{t,i\to i}}{\Delta^h_{t,i\to i} + \Gamma_{t,i} + h(\chi_t, \chi_i; \xi_t, 1)} - \frac{\hat{h}_{t,i\to i}}{\Gamma_{t,i}}\right] + \sum_{k\neq i}\Omega_{t,k}\left[\frac{\hat{h}_{t,i\to i}}{\Delta^h_{t,k\to i} + \Gamma_{t,i} + h(\chi_t, \chi_i; \xi_t, 1)} - \frac{\hat{h}_{t,i\to i}}{\Gamma_{t,i}}\right]\\
&\approx \Omega_{t,i}\left[\frac{\Delta^h_{t,i\to i}}{\Gamma_{t,i}}\right] - \sum_{k\neq i}\Omega_{t,k}\left[\frac{\hat{h}_{t,i\to i}\Delta^h_{t,k\to i}}{\Gamma^2_{t,i}} + \frac{h(\chi_t, \chi_i; \xi_t, 1)\hat{h}_{t,i\to i}}{\Gamma^2_{t,i}}\right]. \qquad (38)
\end{aligned}$$

The approximation (38) holds when

$$\frac{\Gamma_{t,i}}{\Gamma_{t,i} + \Delta^h_{t,k\to i} + h(\chi_t, \chi_i; \xi_t, 1)} \approx 1,$$

which would be true for sufficiently large values of t. Using (38), we upper bound the expected change in local visibility by noting the fact that the expected increase in visibility is the most when the new node has the highest probability to form connection with node i, which occurs when the attribute of the new node is close to χ_i

$$\begin{aligned}
&\mathbb{E}\left[p_i^{\text{local}}(t+1) - p_i^{\text{local}}(t) \mid \mathbb{G}_t, \xi_t, \chi_t\right]\\
&\leq \mathbb{E}\left[p_i^{\text{local}}(t+1) - p_i^{\text{local}}(t) \mid \mathbb{G}_t, \xi_t, \chi_t = \chi_i\right]\\
&\leq \frac{1}{\Gamma_{t,i}}\left[\frac{\hat{h}_{t,i\to i}}{\Gamma_{t,i}}\Delta^h_{t,i\to i} - \sum_{k\neq i}\left(\frac{\hat{h}_{t,k\to i}}{\Gamma_{t,i}}\right)\left(\frac{\hat{h}_{t,i\to i}}{\Gamma_{t,i}}\Delta^h_{t,k\to i} + \frac{h(\chi_t, \chi_i; \xi_t, 1)\hat{h}_{t,i\to i}}{\Gamma_{t,i}}\right)\right] \qquad (39)\\
&\approx \frac{1}{\Gamma^3_{t,i}}\sum_{k\in V_t}\left\{\hat{h}_{t,i\to i}\hat{h}_{t,k\to i}\Delta^h_{t,i\to i} - \hat{h}_{t,i\to i}\hat{h}_{t,k\to i}\Delta^h_{t,k\to i} - \hat{h}_{t,k\to i}\hat{h}_{t,i\to i}h(\chi_i, \chi_i; \xi_t, 1)\right\}\\
&\approx \frac{1}{\Gamma^3_{t,i}}\beta(\xi_i, D_{t-1}(i))\sum_{k\in V_t}\beta(\xi_k, D_{t-1}(k))e^{-\gamma d(\chi_i,\chi_k)} \times \left\{\Delta^h_{t,i\to i} - \Delta^h_{t,k\to i} - \beta(\xi_t, 1)\right\}. \qquad (40)
\end{aligned}$$

Note that the approximation (40) holds when the sum of individual terms for nodes k (in V_t) excluding i is approximately equal to the sum of terms over all nodes. In other words, the approximation holds when

$$\frac{\left(\frac{\hat{h}_{t,i\to i}}{\Gamma_{t,i}}\right)\left(\frac{\hat{h}_{t,i\to i}}{\Gamma_{t,i}}\Delta^h_{t,i\to i} + \frac{h(\chi_t,\chi_i;\xi_t,1)\hat{h}_{t,i\to i}}{\Gamma_{t,i}}\right)}{\sum_{k\neq i}\left(\frac{\hat{h}_{t,k\to i}}{\Gamma_{t,i}}\right)\left(\frac{\hat{h}_{t,i\to i}}{\Gamma_{t,i}}\Delta^h_{t,k\to i} + \frac{h(\chi_t,\chi_i;\xi_t,1)\hat{h}_{t,i\to i}}{\Gamma_{t,i}}\right)} \approx 0,$$

which would be true for sufficiently large values of t. Observe that $\Delta^h_{t,i\to i} = \beta(\xi_i, D_{t-1}(i)+1) - \beta(\xi_i, D_{t-1}(i))$ which equals ξ_i in a multiplicative α model. Similarly, $\Delta^h_{t,k\to i}$ equals $e^{-\gamma d(\chi_i,\chi_k)}\xi_k$. Therefore, in a multiplicative model, (40) reduces to

$$\mathbb{E}\left[p_i^{\text{local}}(t+1) - p_i^{\text{local}}(t) \mid \mathbb{G}_t, \xi_t, \chi_t\right] \lesssim \frac{1}{\Gamma^3_{t,i}}\beta_i(t-1) \times \sum_{k\in V_t}\beta_k(t-1)e^{-\gamma d(\chi_i,\chi_k)}\left\{\xi_i - e^{-\gamma d(\chi_i,\chi_k)}\xi_k - \xi_t\right\}, \qquad (41)$$

which gives the upper bound (36). To lower bound the same, we define the following notation — For $\epsilon > 0$,

$$\chi^{\epsilon}_{i,\min} = \arg\min_{\chi: d(\chi,\chi_i)<\epsilon} \frac{h(\chi_i, \chi; \xi_i, D_i(t))}{\sum_{j\in V_t} h(\chi_j, \chi; \xi_j, D_j(t))}.$$

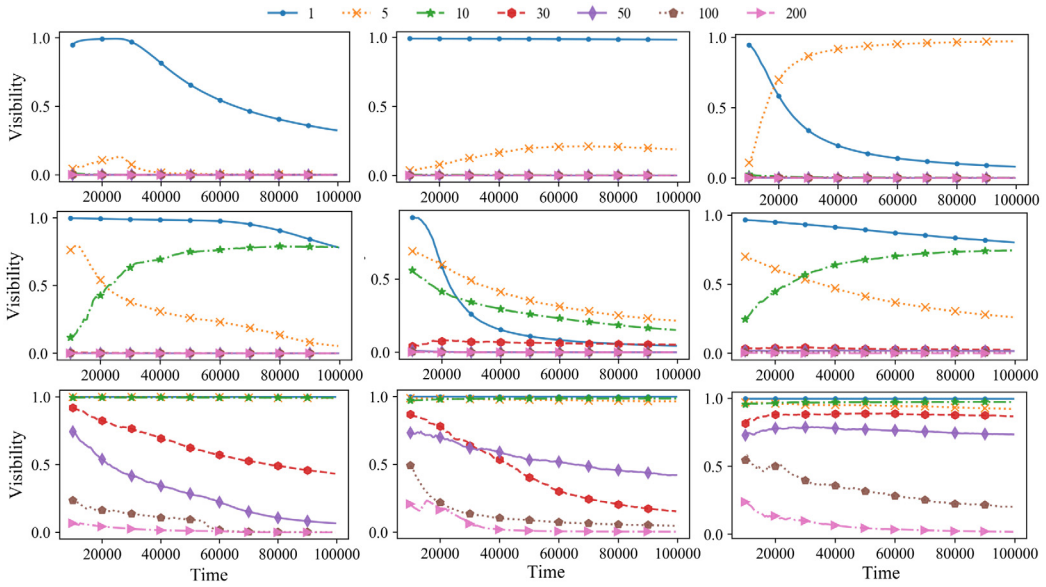

Fig. 4. Visibility of nodes (averaged over 50 independent runs) over time in the spatial growth model, that had the k-highest visibility at time $T_0 = 10000$, for $k = 1, 5, 10, 30, 50, 100, 200$. The columns represent different parameters of the Pareto distribution: $\alpha_p = 1, 2, 3$. Each row shows visibility results for different values of γ parameter, 5, 10 and 50 (from top to bottom). The multiplicative factor $\beta(\xi_i, D_i(t))$ is set to $\xi_i D_i(t)$. Note that more influential nodes emerge for larger values of γ, and they can retain their visibility over longer periods of time for higher values of α_p.

In other words, $\chi^{\epsilon}_{i,\min}$ is the attribute vector on the $\epsilon-$ball around χ_i where the attachment probability to i is the lowest.

Using (38), we lower bound the expected change in local visibility by noting that conditioned on the event that the new node has an attribute vector within an $\epsilon-$ball around χ_i, it will be minimum when it is equal to $\chi^{\epsilon}_{i,\min}$. Accordingly, we define the following notation: $\hat{h}^{\min}_{t,k\to i} = h(\chi_k, \chi^{\epsilon}_{i,min}; \xi_k, D_{t-1}(k))$. We lower bound using conditioning arguments

$$
\begin{aligned}
&\mathbb{E}\left[p_i^{\text{local}}(t+1) - p_i^{\text{local}}(t) \,|\mathbb{G}_t, \xi_t, \chi_t\right] \\
&\geq \mathbb{E}\left[p_i^{\text{local}}(t+1) - p_i^{\text{local}}(t) \;\middle|\; \mathbb{G}_t, \xi_t, d(\chi_t, \chi) < \epsilon\right] \times \mathbf{P}\left[d(\chi_t, \chi) < \epsilon\right] \\
&\geq \mathbb{E}\left[p_i^{\text{local}}(t+1) - p_i^{\text{local}}(t) \;\middle|\; \mathbb{G}_t, \xi_t, \chi_t = \chi^{\epsilon}_{\min}\right] \times \mathbf{P}\left[d(\chi_t, \chi) < \epsilon\right] \\
&\gtrsim \mathbf{P}\left[d(\chi_t, \chi) < \epsilon\right] \cdot \frac{1}{\Gamma^3_{t,i}} \sum_{k\in V_t} \left\{\hat{h}^{\min}_{t,i\to i}\hat{h}_{t,k\to i}\Delta^h_{t,i\to i} - \hat{h}_{t,i\to i}\hat{h}^{\min}_{t,k\to i}\Delta^h_{t,k\to i} - \hat{h}^{\min}_{t,k\to i}\hat{h}_{t,i\to i}h(\chi_i, \chi^{\epsilon}_{i,\min}; \xi_t, 1)\right\} \\
&\gtrsim \mathbf{P}\left[d(\chi_t, \chi) < \epsilon\right] \frac{1}{\Gamma^3_{t,i}} \beta(\xi_i, D_{t-1}(i)) \times \sum_{k\in V_t} \beta_k(t-1) e^{-\gamma d(\chi_i, \chi_k)} \times \left\{e^{-\epsilon\gamma}\xi_i - e^{\epsilon\gamma}e^{-\gamma d(\chi_i,\chi_k)}\xi_k - e^{2\epsilon\gamma}\xi_t\right\},
\end{aligned} \tag{42}
$$

where the final step follows by applying triangle inequality. ■

Also, note that the approximation holds under similar conditions as stated for the proof of the upper bound. From the lower bound (37) it is clear that the visibility will decrease when nodes close to i have high fitness values or the new node has a very high fitness value. The upper bound (36) indicates that if the fitness of node i is sufficiently high compared to other nodes in its local neighborhood, then its visibility should increase. This shows how the local neighborhood of particular node impacts its visibility. Also, given the local nature of the behavior of visibility, more nodes end up being visible in the spatial model compared to the multiplicative fitness model.

6. Experimental results on node visibilities — Spatial models

To illustrate the findings of Section 5.2, we perform experiments discussed in this section. In the previous section, we theoretically argued how the spatial (S) model with multiplicative β would lead to multiple leaders coexisting in the network. Here we present experimental results that show the multiplicity of leaders that can coexist in the network and how this varies with the decay parameter γ. Throughout, the fitness variable ξ is taken to be Pareto distributed (see (27)) with parameter α_p.

For each $\alpha_p = 1, 2, 3$ and $\gamma = 5, 10, 50$, we generate a graph $\mathbb{G}^S_{T_0}$ as an instantiation of the spatial model, with $T_0 = 10000$. We denote $p^{\text{local}}_{(k)}(T_0; \mathbb{G}^S_t)$ to be the local visibility of the node in graph $\mathbb{G}^S_t$ which had the k-highest local

visibility in graph $\mathbb{G}^S_{T_0}$. As previously, we generate R realizations $\mathbb{G}^{S,(1)}_T, \mathbb{G}^{S,(2)}_T, \ldots \mathbb{G}^{S,(R)}_T$ with $T = 100000$, which are mutually independent conditioned on $\mathbb{G}^S_{T_0}$. We average the local visibility values across all the realizations at any given time and denote $\bar{p}^{\text{local}}_{(k)}(T_0; t; S) = \frac{1}{R}\sum_{r=1}^{R} p^{\text{local}}_{(k)}(T_0; \mathbb{G}^{S,(r)}_t)$ as the averaged local visibility of the node at time t which had the k-highest visibility at time T_0 for the spatial model.

In other words, we track $p^{\text{local}}_{(k)}\left(T_0; \mathbb{G}^{S,(r)}_t\right)$ for nodes $k = 1, 5, 10, 30, 50, 100, 200$, runs $r = 1, 2, \ldots, R$, and decay parameters $\gamma = 5, 10, 50$, with $10000 \le t \le 100000$. Observe that the local visibility values of nodes are bounded above by 1, but they could sum up to values larger than 1. This is an artifact of the way local visibility is defined. Lemma 5.2 gives the relationship between the concept of local visibility and global visibility (which is the actual probability of connection to the concerned node). An easy way of deriving the approximate probability of attachment to a particular node i is to consider the domain of attraction around the node. We can define the domain of attraction of node i as the region in the location space such that the distance factor $\alpha(\cdot,\cdot)$ is at least $\frac{1}{e}$. The probability that a new node arises in the domain of attraction of node i is $\frac{\pi}{\gamma^2}$. Therefore an approximation of node visibility that is normalized across the network is $\frac{\pi}{\gamma^2} p_i^{local}(t+1)$.

Fig. 4 shows the change in local visibility of top kth nodes at $t = T_0 = 10000$ when the graph is allowed to grow for 90000 iterations until $t = 100000$. Visibility values averaged over $R = 50$ independent runs from $T_0 = 10000$ are shown. We observe that with increasing γ, the number of nodes with high local visibility increases in the network. This corroborates the insight that with increasing γ, the region of influence of nodes decreases leading to the potential of larger number of influential nodes in the network. For $\gamma = 5$ and $\alpha_p = 1$, we see that the $k = 5$th node increases slightly in visibility beyond $t = 10000$ but then decays beyond a certain point; and with $\alpha_p = 2$, the same node maintains its visibility until $t = 100000$, while for $\alpha_p = 3$ the node increases its local visibility and dominates its region eventually. However for $k = 10, 30, \ldots$, the corresponding nodes have very low values of local visibility. This changes for the $\gamma = 10$ case. Here, the $k = 10$th node also shows a high value of local visibility due to the reduced region of influence of nearby influential nodes. This becomes even more pronounced in $\gamma = 50$ where we observe that even the $k = 200$th node has non-trivial local visibility values that are maintained over some period of time for $\alpha_p = 2, 3$. This shows that with increasing the decay parameter of the spatial model we can significantly increase the number of leaders in the network, many of whom can maintain their influence in their region.

7. Conclusion

In this paper, we first defined the concept of node visibility, and analyzed the visibility profile of nodes in the context of various network growth models. Firstly, we observed that in the multiplicative fitness model, nodes with high fitness values can successfully maintain visibility in the network to a greater extent when compared with the additive fitness and BA models. A general fitness model that has a non-linear attachment rule, e.g., that combines the degree and fitness values in a non-linear (quadratic) fashion, would also allow influential nodes to maintain visibility. However, unlike in multiplicative models, in these general fitness models with non-linear attachment rules we showed that it becomes progressively more difficult for new nodes with high fitness values to become influential in the entire network. We demonstrated through experimental results that in multiplicative models only a few number of nodes can be influential in the network at any given moment of time. This leads us to investigate spatial models that allows a multiplicity of influential nodes to exist in the network. We also show how the decay parameter in these spatial models can be used to control the number of leaders in the network. Throughout, we describe conditions under which influential nodes might maintain or increase their visibility over time.

CRediT authorship contribution statement

Shravika Mittal: Methodology, Software, Validation, Visualization, Writing – original draft, Writing – review & editing. **Tanmoy Chakraborty:** Conceptualization, Validation, Writing – original draft, Supervision, Project administration. **Siddharth Pal:** Conceptualization, Methodology, Validation, Formal analysis, Writing – original draft, Writing – review & editing.

Declaration of competing interest

The authors declare that they have no known competing financial interests or personal relationships that could have appeared to influence the work reported in this paper.

Acknowledgments

The authors would like to thank Dr. Ralucca Gera at Naval Postgraduate School, and Dr. Soham De at DeepMind, for insightful discussions and collaboration on previous works that led to this paper.

References

[1] M. Newman, Networks: An Introduction, Oxford University Press, 2010.
[2] M. Newman, The structure and function of complex networks, SIAM Rev. 45 (2) (2003) 167–256.
[3] D. Wang, C. Song, A.-L. Barabási, Quantifying long-term scientific impact, Science 342 (6154) (2013) 127–132.
[4] T. Chakraborty, S. Kumar, P. Goyal, N. Ganguly, A. Mukherjee, On the categorization of scientific citation profiles in computer science, Commun. ACM 58 (9) (2015) 82–90.
[5] D. Chen, L. Lü, M.-S. Shang, Y.-C. Zhang, T. Zhou, Identifying influential nodes in complex networks, Physica A 391 (4) (2012) 1777–1787, http://dx.doi.org/10.1016/j.physa.2011.09.017, URL http://www.sciencedirect.com/science/article/pii/S0378437111007333.
[6] C. Guo, L. Yang, X. Chen, D. Chen, H. Gao, J. Ma, Influential nodes identification in complex networks via information entropy, Entropy 22 (2) (2020) 242, http://dx.doi.org/10.3390/e22020242, URL http://dx.doi.org/10.3390/e22020242.
[7] M. Kimura, K. Saito, R. Nakano, Extracting influential nodes for information diffusion on a social network, in: Proceedings of the 22nd National Conference on Artificial Intelligence - Volume 2, AAAI'07, AAAI Press, 2007, pp. 1371–1376.
[8] A.-L. Barabási, Scale-free networks: a decade and beyond, Science 325 (5939) (2009) 412–413, http://dx.doi.org/10.1126/science.1173299.
[9] A.-L. Barabási, R. Albert, Emergence of scaling in random networks, Science 286 (5439) (1999) 509–512.
[10] A. Noulas, B. Shaw, R. Lambiotte, C. Mascolo, Topological properties and temporal dynamics of place networks in urban environments, in: Proceedings of the 24th International Conference on World Wide Web, 2015, pp. 431–441.
[11] T. Chakraborty, S. Nandi, Universal trajectories of scientific success, Knowl. Inf. Syst. 54 (2) (2018) 487–509, http://dx.doi.org/10.1007/s10115-017-1080-y, URL https://doi.org/10.1007/s10115-017-1080-y.
[12] D. Mohapatra, S. Pal, S. De, P. Kumaraguru, T. Chakraborty, Modeling citation trajectories of scientific papers, in: Advances in Knowledge Discovery and Data Mining - PAKDD'20, 2020, pp. 620–632.
[13] L. Adamic, B. Huberman, Power-law distribution of the world wide web, Science 287 (2000) 2115.
[14] J. Kong, N. Sarshar, V. Roychowdhury, Experience versus talent shapes the structure of the web, Proc. Natl. Acad. Sci. 105 (37) (2008) 13724–13729, http://dx.doi.org/10.1073/pnas.0805921105, URL http://dx.doi.org/10.1073/pnas.0805921105.
[15] D. Amancio, O. Oliveira, L. da Fontoura Costa, Three-feature model to reproduce the topology of citation networks and the effects from authors' visibility on their h-index, J. Informetr. 6 (3) (2012) 427–434, http://dx.doi.org/10.1016/j.joi.2012.02.005, URL http://www.sciencedirect.com/science/article/pii/S1751157712000211.
[16] G. Bianconi, A.-L. Barabási, Bose-Einstein condensation in complex networks, Phys. Rev. Lett. 86 (24) (2001) 5632.
[17] G. Bianconi, A.-L. Barabási, Competition and multiscaling in evolving networks, Europhys. Lett. 54 (4) (2001) 436–442, http://dx.doi.org/10.1209/epl/i2001-00260-6.
[18] K. Nguyen, D. Tran, Fitness-based generative models for power-law networks, in: M.T. Thai, P.M. Pardalos (Eds.), Handbook of Optimization in Complex Networks: Theory and Applications, Springer US, Boston, MA, 2012, pp. 39–53, http://dx.doi.org/10.1007/978-1-4614-0754-6_2.
[19] G. Caldarelli, A. Capocci, P. De Los Rios, M.A. Muñoz, Scale-free networks from varying vertex intrinsic fitness, Phys. Rev. Lett. 89 (2002) 258702, http://dx.doi.org/10.1103/PhysRevLett.89.258702, URL https://link.aps.org/doi/10.1103/PhysRevLett.89.258702.
[20] D. Garlaschelli, M. Loffredo, Fitness-dependent topological properties of the world trade web, Phys. Rev. Lett. 93 (2004) 188701, http://dx.doi.org/10.1103/PhysRevLett.93.188701, URL https://link.aps.org/doi/10.1103/PhysRevLett.93.188701.
[21] D. Tsiotas, Detecting differences in the topology of scale-free networks grown under time-dynamic topological fitness, Sci. Rep. 10 (1) (2020) 10630, http://dx.doi.org/10.1038/s41598-020-67156-6, URL https://doi.org/10.1038/s41598-020-67156-6.
[22] M. Bell, S. Perera, M. Piraveenan, M. Bliemer, T. Latty, C. Reid, Network growth models: A behavioural basis for attachment proportional to fitness, Sci. Rep. 7 (1) (2017) 42431, http://dx.doi.org/10.1038/srep42431, URL https://doi.org/10.1038/srep42431.
[23] M. Kii, K. Akimoto, K. Doi, Random-growth urban model with geographical fitness, Physica A 391 (23) (2012) 5960–5970, http://dx.doi.org/10.1016/j.physa.2012.07.033, URL https://www.sciencedirect.com/science/article/pii/S0378437112007029.
[24] G. Ergün, G. Rodgers, Growing random networks with fitness, Physica A 303 (1) (2002) 261–272.
[25] E. Bullmore, O. Sporns, Complex brain networks: graph theoretical analysis of structural and functional systems, Nat. Rev. Neurosci. 10 (3) (2009) 186–198, http://dx.doi.org/10.1038/nrn2575, URL https://doi.org/10.1038/nrn2575.
[26] M. Allamanis, S. Scellato, C. Mascolo, Evolution of a location-based online social network: Analysis and models, in: Proceedings of the Internet Measurement Conference, 2012, pp. 145–158.
[27] D. Liu, V. Fodor, L. Rasmussen, Will scale-free popularity develop scale-free geo-social networks? IEEE Trans. Netw. Sci. Eng. 6 (3) (2019) 587–598.
[28] R. Guimerá, L. Amaral, Modeling the world-wide airport network, Eur. Phys. J. B 38 (2) (2004) 381–385, http://dx.doi.org/10.1140/epjb/e2004-00131-0, URL https://doi.org/10.1140/epjb/e2004-00131-0.
[29] S.-H. Yook, H. Jeong, A.-L. Barabási, Modeling the Internet's large-scale topology, Proc. Natl. Acad. Sci. 99 (21) (2002) 13382–13386.
[30] M. Kaiser, C. Hilgetag, Spatial growth of real-world networks, Phys. Rev. E 69 (3) (2004) http://dx.doi.org/10.1103/physreve.69.036103, URL http://dx.doi.org/10.1103/PhysRevE.69.036103.
[31] M. Barthélemy, Crossover from scale-free to spatial networks, Europhys. Lett. 63 (6) (2003) 915.
[32] M. Barthélemy, Spatial networks, Phys. Rep. 499 (1–3) (2011) 1–101, http://dx.doi.org/10.1016/j.physrep.2010.11.002, URL http://dx.doi.org/10.1016/j.physrep.2010.11.002.
[33] V. Servedio, G. Caldarelli, P. Buttà, Vertex intrinsic fitness: How to produce arbitrary scale-free networks, Phys. Rev. E 70 (5) (2004) 056126.
[34] S. Pal, S. De, T. Chakraborty, R. Gera, Visibility of nodes in network growth models, in: 3rd International Winter School and Conference on Network Science, 2017, pp. 35–45.
[35] P.L. Krapivsky, S. Redner, Organization of growing random networks, Phys. Rev. E 63 (6) (2001) 066123.
[36] M. Mitzenmacher, A brief history of generative models for power law and lognormal distributions, Internet Math. 1 (2) (2004) 226–251.
[37] L. Ferretti, M. Cortelezzi, Preferential attachment in growing spatial networks, Phys. Rev. E 84 (1) (2011) http://dx.doi.org/10.1103/physreve.84.016103, URL http://dx.doi.org/10.1103/PhysRevE.84.016103.
[38] G. Caldarelli, A. Capocci, P. De Los Rios, M.A. Muñoz, Scale-free networks from varying vertex intrinsic fitness, Phys. Rev. Lett. 89 (25) (2002) 258702.